New Journal of Physics
The open-access journal for physics

Spatially resolved measurement of ionization yields in the focus of an intense laser pulse

M Schultze[1,2,3], B Bergues[1], H Schröder[1], F Krausz[1,2] and K L Kompa[1]

[1] Max-Planck-Institut für Quantenoptik, Hans-Kopfermann-Strasse 1, D-85748 Garching, Germany

[2] Ludwig-Maximilians-Universität München, Fakultät für Physik, Am Coulombwall 1, D-85748 Garching, Germany

E-mail: martin.schultze@mpq.mpg.de

New Journal of Physics **13** (2011) 033001 (9pp)
Received 29 August 2010
Published 1 March 2011
Online at http://www.njp.org/
doi:10.1088/1367-2630/13/3/033001

Abstract. We introduce a novel technique for measuring spatially resolved photoionization yields of gas-phase ions created in an intense-laser focus. Overcoming the limitations of traditional experiments where the ionization yield is integrated over the entire focal volume, the technique provides precise information on the ionization dynamics over a wide range of intensities between the appearance intensity of the lowest charge state up to relativistic intensities. The new method provides insights into the ionization process beyond the saturation intensity and, at the same time, a precise way for noninvasive, *in situ* focus diagnostics. We demonstrate these advances for the case of strong-field ionization of argon. The data are analyzed using the Ammosov–Delone–Krainov (ADK) formula (Ammosov *et al* 1986 *Zh. Éksp. Teor. Fiz.* **91** 2008).

The development of ultrashort and super-intense laser sources in recent decades has allowed the study of atomic and molecular dynamics in electromagnetic fields with field strengths comparable to or higher than the field binding the electron to the proton in the ground state of the hydrogen atom. Exposing atoms to such high field strengths is today routinely achieved in laboratories by focusing ultrashort laser pulses into a gas target. Information about the target dynamics can be gained by detecting the ions or electrons emitted in the laser focus. The results of such studies have been reported in numerous publications [2].

In a standard experiment, particles are collected over the whole focal volume and recorded as a function of the peak intensity I_0 in the focus. The ion yield $Y_{\mathrm{tot}}(I_0)$ measured in such an

[3] Author to whom any correspondence should be addressed.

experiment is thus a convolution of the intensity-dependent yield $Y(I)$—where I is the local peak intensity of the pulse—with the focal intensity distribution $K(I, I_0)$:

$$Y_{\mathrm{tot}}(I_0) = \int_0^{I_0} Y(I)\,K(I, I_0)\,\mathrm{d}I. \tag{1}$$

It should be emphasized that under real experimental conditions $K(I, I_0)$ should also account for effects such as beam imperfections, diffraction or aberrations of the focusing optics. The measured yield is thus dependent on the particular focus geometry, and the focal intensity distribution itself is a function of the global peak intensity. An additional complication encountered in standard experiments results from the fact that the intensity I_0 is varied using an attenuator, which in general is not diffraction and dispersion free and thus affects the pulse shape and focus geometry. This is especially relevant for experiments with ultrashort laser pulses where broadband and dispersion-free optics are required.

A consequence of equation (1) is that meaningful comparisons of experimental results with theoretical models (as for instance [1, 3]) clearly require a precise knowledge of the spatiotemporal intensity distribution in the detection volume. While the temporal shape of a short laser pulse can be determined very precisely [4], the spatial intensity distribution in the focus is in general a subject of speculation and difficult to reconstruct based on measurements. Established techniques for laser-focus diagnostics such as the knife-edge method and optical imaging require additional optics and thus suffer from diffraction and aberration introduced by the diagnostics themselves. Since their resolution is subjected to the diffraction limit, these techniques are inherently incapable of resolving local intensity modulations on a wavelength scale, which is characteristic for interference structures. It should be noted that the common assumption of Gaussian focusing with smooth intensity distributions is a great oversimplification.

Averaging ion yields over the focal volume leads to a loss of information. Due to the inherent noise in experimental data, convolution (1) can mask important features of the yield curve $Y(I)$, even if the focal intensity distribution known exactly. The most evident example is the expected decrease of $Y(I)$ beyond the saturation intensity that occurs when the population of the measured charge state is depleted via ionization to a higher charge state. This effect is not observed in traditional experiments. Focal averaging, together with an inaccurate characterization of the focal intensity distribution, thus often hinders quantitative analysis of multi-photon or intense field photoionization data (see for instance the interpretation of the challenging results recently obtained at FLASH [5]–[7]).

The only way to reduce the loss of information is to reduce the number of spatial dimensions over which the ion yield is integrated and, ideally, spatially resolve the ion yield in all three dimensions. A first step in this direction was achieved with the method originally introduced by Schröder *et al* [8] and that became popular under the name 'intensity selective scanning' (ISS) [9]. In such experiments, the detection volume is confined in a plane perpendicular to the laser propagation axis z by a small entrance slit in front of the time-of-flight (TOF) spectrometer. The intensity is then varied by scanning the entrance slit along the z-axis and the ionization yield collected as a function of the position z. The drawback of this method is that the ion yield is still integrated over two dimensions and that separate focus diagnostics are required to calibrate the intensity dependence. Other techniques that suffer from similar problems [10] or that lack sufficient resolution [11, 12] have been reported over the last few years. Experiments that tackle the problem of volume averaging have attracted a wide interest in the intense field physics community. Two recent studies on strong-field ionization of argon [13]

and xenon [14] suggest the persistence of singly charged ions even in the most intense part of the laser focus.

We report here on two methods that both allow the measurement of spatially resolved ionization yields in all three dimensions and, at the same time, provide access to noninvasive, *in situ* focus diagnostics. The first method is based on a reflectron TOF spectrometer (R-TOF) technique [15, 16] and resembles the approach presented in [14], with the main difference being that our method provides constant spatial resolution for ions in different charge states and directly yields their relative amount. We then discuss a second method that follows a completely different approach based on a novel imaging technique, which we termed 'ion microscopy'.

For our studies we employed linearly polarized laser pulses with a central wavelength of 780 nm, a pulse energy of 1.5 mJ and a duration τ of 48 fs (full-width at half-maximum (FWHM) in intensity) generated in a Ti:sapphire laser system with a repetition rate of 1 kHz. An achromatic doublet with a focal length of 15 cm was used to focus the laser beam into the center of the experimental chamber, between the repeller and the extractor electrode of the R-TOF. The chamber was filled with argon at a pressure of 3×10^{-7} mbar, low enough to avoid space-charge effects. The pressure of the residual background was 2×10^{-8} mbar.

Ions created in the laser focus are accelerated in the positive x-direction by a homogeneous electric field applied between the repeller and the extractor electrode, as depicted in figure 1(a). An entrance aperture of 10 μm diameter in the extractor confines the detection volume to a small cylinder with symmetry axis perpendicular to the laser propagation direction (z-direction). Ions passing the aperture reach a four-grid arrangement reflector and are redirected towards a detector consisting of a multi-channel plate (MCP) that is run in the current mode. The TOF spectrum is integrated over 1000 laser shots and recorded using an averaging oscilloscope.

Because of the steep potential gradient in the x-direction between repeller and extractor, the x-position of an ion at the instant of its birth in the laser focus is proportional to the kinetic energy it has gained when passing the entrance aperture. By using the reflector as an energy filter [15] to select ions with kinetic energies within a certain energy interval, we are able to further confine the detection volume to 13 μm along the x-direction. Ions with a kinetic energy above this energy interval are not recorded. Those with a kinetic energy below the energy interval reach the detector at earlier times, forming a 'peripheral' peak in the TOF spectrum. Ions with a kinetic energy within the energy interval constitute the 'confined' peak that contains only signal from ions created in the cylindrical detection volume of 13 μm length and 10 μm diameter.

In figure 1(b), we present the TOF spectrum of ions generated in the most intense region of the laser focus. The spectrum shows contributions of argon charge-states up to Ar^{6+}. The splitting of the peaks into 'peripheral' and 'confined' peaks is highlighted in the inset to figure 1(b) using the example of Ar^{3+}. One can see that charge states higher than Ar^{4+} are created only inside the detection volume (there is no peripheral peak), while for lower charge states the major contribution originates from regions outside the detection volume, which results in a dominant peripheral peak. For the laser parameters used in the present experiment, the predominant charge state is Ar^{5+}. An important feature of our detection scheme is that it detects all charge states and species in a single shot with practically the same detection efficiency. We thus obtain accurate ionic charge state distributions that are, to a large extent, free of volume averaging.

In order to explore the influence of intensity on ionization yields and charge state distribution, we recorded R-TOF spectra over a wide range of quasi-isolated intensities by

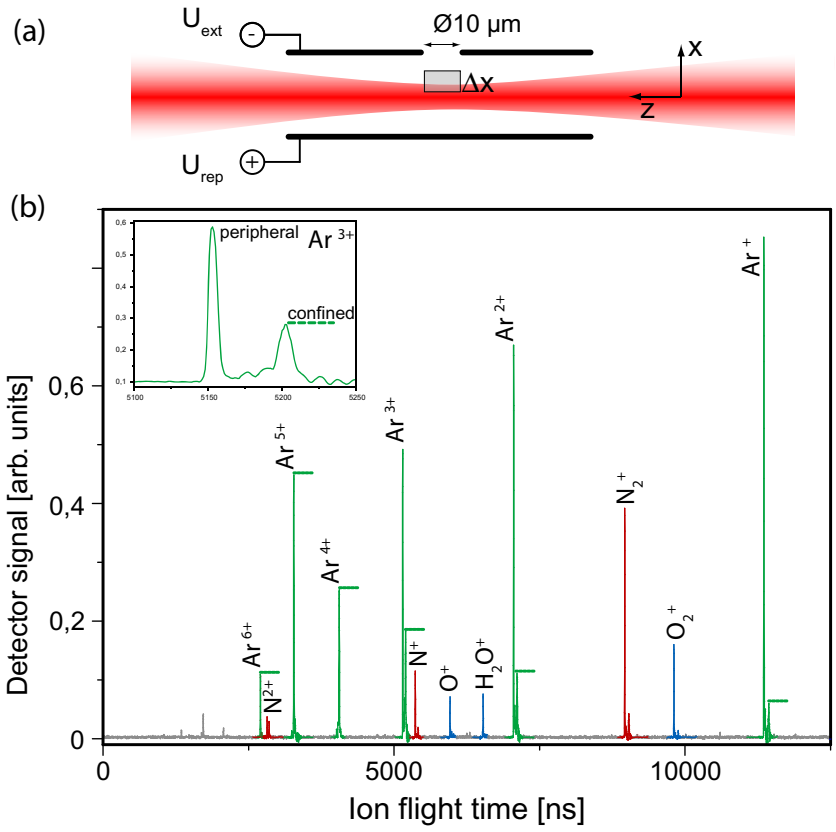

Figure 1. (a) Sketch of the detection volume in the reflectron spectrometer. (b) TOF spectrum obtained by ionization of argon in the most intense part of the focal volume at a peak intensity of $7.4 \times 10^{15}\,\mathrm{W\,cm^{-2}}$. Ions that are created inside a cylindrical volume of 10 μm diameter and 13 μm length constitute a separate ('confined') TOF peak. The second ('peripheral') peak originates from ions generated outside the detection volume. The inset shows that about one out of three triply ionized argon ions originates from the small confined volume, and the higher charged ions are exclusively created inside the confined volume. Residual gas inside the experimental chamber (mostly nitrogen and water) is ionized as well and the charged fragments appear in the flight time spectrum. Despite the orders of magnitude lower partial pressure, they occur as prominent peaks because of their lower ionization potential.

mechanically shifting the focus position along the x-direction, i.e. by scanning the detection volume across the laser focus. The dependence of the ionization yields on the x-coordinate ($x = 0$ corresponds to the center of the focus) is shown in figure 2 for Ar^{1+} to Ar^{6+}. When the detection volume is moved towards the center of the focus to probe higher intensities, the ionization yields first increase. For the lowest charged states (Ar^{1+} to Ar^{4+}), however, we observe saturation of the ionization process at well-defined intensities when approaching the $x = 0$ position. Beyond the saturation intensity the population of these lower charge states is depleted via ionization to higher charge states.

In order to develop a more quantitative understanding of our data, we present the comparison of our experimental results with the predictions (see figure 2) of the ADK

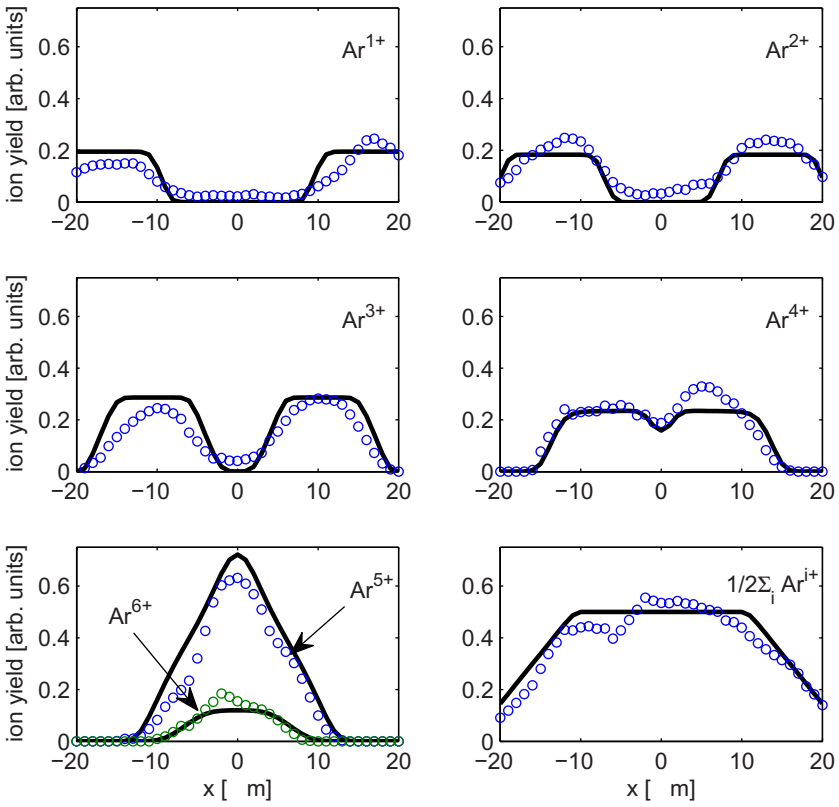

Figure 2. Circles: dependence of Ar^{1+} to Ar^{6+} ionization yields on the distance of the detection volume from the beam axis. The onion shell-like structure of the lower charged states reveals their depletion in favor of higher charged states with increasing intensities. Solid line: predictions of the Ammosov–Delone–Krainov (ADK) model.

formula [1], which is a special case of the theory presented in [17] applicable for tunneling ionization. To simplify the analysis we assume a Gaussian intensity dependence along the x- and y-directions and a sine-square envelope for the time evolution of the electric field to describe the laser pulse. Best agreement between theory and experiment is obtained for a peak intensity of 7.4×10^{15} W cm^{-2} and a focal width of 15 μm FWHM in intensity. The finite spatial resolution in x- and y-directions is accounted for in the simulation.

Given the simplicity of the model and the approximations made for the focal geometry, the agreement between the experimental data and theoretical results shown in figure 2 is quite impressive. The signal amplitude as well as the saturation intensities predicted for the different charge states are fairly consistent with the measured data. The remaining discrepancies reveal that the focal geometry is far more complex than is assumed in the calculation. This is expressed in the asymmetry the measured curves exhibit between the contributions from the two sides of the focus. The strongest mismatch between experiment and simulation is observed in the Ar^{1+} signal that mainly probes the outer part (at large $|x|$) of the focal volume. This is not unexpected, since aberration-induced deviations from the Gaussian geometry are usually most pronounced in the periphery of the focus.

A striking feature of the experimental data is the presence of Ar^{1+} in the center of the focus, although Ar^{6+} ions are generated in this region. In contrast to the result of the ADK model that

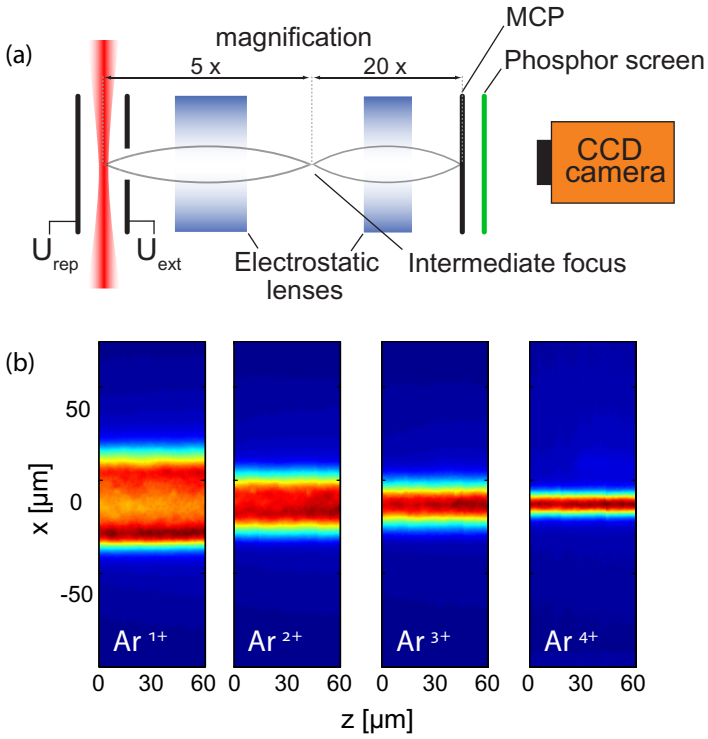

Figure 3. (a) Schematic view of the ion microscope. (b) False color raw images of the charge states Ar^{1+} to Ar^{4+} as recorded with the ion microscope at the beam waist. The images were recorded over 60 000 laser shots.

predicts the absence of singly charged argon ions in the center of the focus, we observe a ratio between Ar^{1+} and Ar^{5+} of 1 to 35. This finding might be attributed to processes competing with ionization, such as harmonic generation [18] or frustrated tunneling [19]. Note that this signal could not be reproduced by varying the size of the detection volume used in the simulation within experimental uncertainty.

While a great advantage of the R-TOF method is that the charge state distribution in the detection volume is recorded in a single shot, it also has some limitations. Fast focus diagnostics are hampered by the need to scan the detection volume in all three dimensions. The spatial resolution that can be achieved is ultimately limited by the size of the entrance aperture. Decreasing the aperture size below 10 μm would, however, drastically increase the acquisition time due to the low statistics. As a consequence, slow drifts of the laser parameters might affect the data.

Most of these limitations are overcome with our novel ion microscopy technique. In the ion microscope, the ion distribution in the laser focus (located in the object plane) is mapped onto a position-sensitive detector located in the image plane. As opposed to a velocity mapping spectrometer that images the momentum distribution of the charged particles, the ion microscope reveals their spatial distribution. A schematic view of the device that was developed in collaboration with Stefan Käsdorf [20] is presented in figure 3(a). Ions generated in the laser focus are first accelerated by an electric field applied between repeller and extractor electrodes. A first electrostatic lens images the spatial extent of the ion cloud into the ion microscope with a small magnification factor. This intermediate image is located in the focal plane of a second

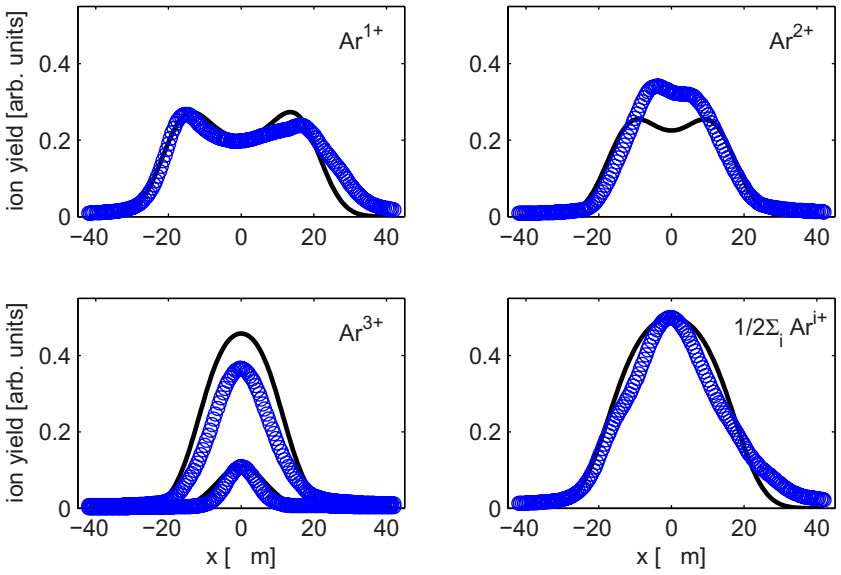

Figure 4. Circles: x-dependence of the Ar^{1+} to Ar^{4+} signals obtained after integration of the raw images along the propagation direction. Solid line: predictions of the ADK model.

electrostatic lens that projects a further magnified image onto the detector consisting of a pair of MCPs and a phosphor screen. The image of the ion cloud that appears on the phosphor screen is recorded with a CCD camera. It represents a magnified orthogonal projection (along the y-axis) of the focal ion distribution under scrutiny. Since fragments with different charge to mass ratios have different flight times, gating the detector with a 7 ns time window enables us to mass select individual charge states. In case the ion distribution is symmetric under rotation about the beam propagation axis, the full three-dimensional (3D) distribution can be recovered via Abel inversion of the raw images. With the present device, a magnification of about 100 and a resolution better than 4 μm have been achieved. While different charge states have to be recorded sequentially, all ions (with the same charge to mass ratio) that are created in the focal volume are collected in a single acquisition. This results in a considerably higher signal than for scanning techniques and renders focus imaging within a few minutes. Technically, sub-micron spatial resolution should be possible.

Ion microscopy is a powerful method to characterize focal geometries. At this point we would like to stress that it represents a considerable improvement on conventional ISS techniques, since it additionally determines the beam diameter along the propagation direction, whereas ISS and its successors have to rely on speculations regarding the focus geometry.

In order to explore the potential of the ion microscope, we repeated the strong field photoionization experiment described above. Apart from the focusing (here we used a lens with 22 cm focal length), the experimental conditions were similar to those used in the R-TOF experiment. Raw images of the charge states Ar^{1+} to Ar^{4+} are shown in figure 3(b) . An area of 170 μm (perpendicular to the beam axis) times 60 μm along the beam propagation direction was imaged onto the detector. Since 60 μm corresponds to only a small fraction of the Rayleigh range, the acquired signal exhibited no z-dependence. For a quantitative analysis analogue to the one performed for the R-TOF data, we summed up the signal along z. The resulting spatial dependence of the ion signal is represented in figure 4, together with the results of an ADK

simulation. The best agreement was achieved where a peak intensity of 3.1×10^{15} W cm^{-2} and a focal width of 20 μm (FWHM) were used as fitting parameters.

Here, our ability to 'look inside' the laser focus again reveals the extent to which the spatial intensity dependence in the outer region of the focus differs from that of the Gaussian dependence that is commonly assumed. In spite of the lower peak intensity used in this experiment, the data recorded with the ion microscope exhibited qualitatively the same features as those presented in figure 2. In particular, the depletion of the Ar^{1+} and Ar^{2+} ion population in the center of the focus was observed. Given the asymmetry of the focal ion distributions, Abel inversion cannot reliably be applied in the present case. Instead, projections of the ion distributions predicted by theory are displayed. Apart from deviations in the signal heights, we observe reasonable qualitative agreement between experimental results and the predictions of the ADK model. For quantitative conclusions, however, further investigations are required to safely exclude artifacts in the ion images.

In conclusion, we have reported on different techniques to measure spatially resolved yields of ions created in the focus of an intense laser pulse. We were able to study the behavior of ionization beyond the saturation intensity and could directly observe the depletion of lower charge states in favor of the creation of higher charged ions. Our method thus extends the experimentally accessible parameter space, allowing us to refine theoretical models by virtue of this additional information. A fairly good agreement was found between experimental results and the predictions of the ADK model. Further investigations are needed, however, to determine the exact origin of the remaining discrepancies between theory and experiment. Our studies revealed the presence of singly charged argon ions even in the most intense part of the laser focus where the local intensity overcomes the saturation intensity by a factor of 15, as witnessed by the generation of Ar^{6+} in the same volume. This effect might be attributed to HHG [18] or to the population of excited states [19].

We aim to improve the spatial resolution of the present device to the sub-micrometer scale in order to apply our technique to inspect the structure of focused VUV pulses. Melioration of the TOF discrimination will give direct access to arbitrary 3D ion distribution by slicing the focal volume along the x-direction. The techniques introduced and their development thus pave the way for high resolution and truly intensity-resolved photoionization studies, which are essential to uncover subtle effects and further stimulate the development of photoionization theories.

Acknowledgment

We greatly appreciate continuous technical support from Walter Ritt.

References

[1] Ammosov M V, Delone N B and Krainov V P 1986 *Zh. Éksp. Teor. Fiz.* **91** 2008
[2] Posthumus J H 2004 *Rep. Prog. Phys.* **67** 623
[3] Uiterwaal C J G J, Gebhardt C R, Schröder H and Kompa K-L 2004 *Eur. Phys. J.* D **30** 379–92
[4] Trebino R 2002 *Frequency-Resolved Optical Gating: The Measurement of Ultrashort Laser Pulses* (Berlin: Springer)
[5] Sorokin A A *et al* 2007 *Phys. Rev. Lett.* **99** 213002
[6] Makris M G *et al* 2009 *Phys. Rev. Lett.* **102** 033002

[7] Richter M *et al* 2009 *Phys. Rev. Lett.* **102** 163002
[8] Wagner M and Schröder H 1993 *Int. J. Mass Spectrom. Ion Processes* **128** 31–45
[9] Hansch P, Walker M A and Van Woerkom L D 1996 *Phys. Rev.* A **54** R2559
[10] Bryan W A *et al* 2006 *Phys. Rev.* A **73** 013407
[11] Bredy R *et al* 2004 *J. Opt. Soc. Am.* B **21** 2221
[12] Jones R R 1995 *Phys. Rev. Lett.* **74** 1091
[13] Bryan W A *et al* 2006 *Nat. Phys.* **2** 379–83
[14] Strohaber J and Uiterwaal C J G J 2008 *Phys. Rev. Lett.* **100** 023002
[15] Wagner M and Schröder H 1993 *Int. J. Mass Spectrom. Ion Process.* **128** 31
[16] Witzel B *et al* 1998 *Int. J. Mass Spectrom. Ion Process.* **172** 229
[17] Perelomov A M, Popov V S and Terent'ev M V 1966 *Zh. Eksp. Teor. Fiz.* **50** 1393
Perelomov A M, Popov V S and Terent'ev M V 1966 *Zh. Eksp. Teor. Fiz.* **51** 309
Perelomov A M, Popov V S and Terent'ev M V 1966 *Sov. Phys.— JETP* **23** 924
Perelomov A M, Popov V S and Terent'ev M V 1967 *Sov. Phys.— JETP* **24** 207
[18] David Gaudiosi M *et al* 2006 *Phys. Rev. Lett.* **96** 203001
[19] Nubbemeyer T, Gorling K, Saenz A, Eichmann U and Sandner W 2008 *Phys. Rev. Lett.* **101** 233001
[20] Kaesdorf S Geräte für Forschung und Industrie, Gabelsbergerstr. 59 D-80333 München, Germany